

KERNFORSCHUNGSZENTRUM

KARLSRUHE

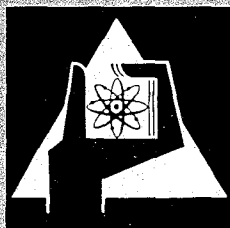
August 1967

KFK 649

Institut für Angewandte Reaktorphysik

Recent Developments in the SEFOR Experimental Program

L. Noble, G.R. Pflasterer, C.D. Wilkinson, L. Caldarola



GESELLSCHAFT FÜR KERNFORSCHUNG M. B. H.

KARLSRUHE

August 1967

K F K 649

Institut für Angewandte Reaktorphysik

RECENT DEVELOPMENTS IN THE SEFOR EXPERIMENTAL PROGRAM*

by

L. Noble**

G. R. Pflasterer**

C. D. Wilkinson**

L. Caldarola***

Gesellschaft für Kernforschung m.b.H., Karlsruhe

* Work performed within the association in the field of fast reactors between the European Atomic Energy Community and Gesellschaft für Kernforschung m.b.H., Karlsruhe, and presented to the International Conference on Critical Experiments and Their Analysis, Argonne National Laboratory, Argonne, Illinois, October 10-13, 1966.

** Advanced Products Operation, General Electric Company, San José, California.

*** EURATOM, Brussels, delegated to the Karlsruhe Fast Breeder Project, Institut für Angewandte Reaktorphysik, Kernforschungszentrum, Karlsruhe.

Executive Summary

Financial Performance

Revenue increased by 10% compared to the previous year, while expenses remained relatively stable. The net profit margin improved from 15% to 18%.

Operational Efficiency

The company successfully implemented a new project management system, resulting in a 15% reduction in project completion time and a 10% decrease in budget overruns.

Customer satisfaction scores improved significantly, with a 20% increase in the number of repeat customers. This was achieved through enhanced customer service training and streamlined processes.

ABSTRACT

The objective of the SEFOR experimental program is to obtain reactivity coefficient information that can be used to predict with confidence the kinetic behaviour of large fast ceramic reactors. In order to obtain this information, three types of experiments will be performed: (1) static tests, (2) oscillator tests, and (3) transient (including super-prompt critical) tests.

In the static tests, the power, flow, and inlet temperature can be changed in such a way that the reactivity effect associated with a change in fuel temperature due to power only, the coolant temperature coefficient, the combined power and temperature coefficient, and the flow coefficient can be determined.

Three types of oscillator tests have been analyzed.

1. The conventional oscillator tests in which the reactivity-power transfer function due to the oscillation of a poison rod is determined.
2. Balanced oscillator tests in which the reactivity-power transfer function is determined for the case in which the relative phase and amplitude of a reactivity oscillation and a flow oscillation are adjusted so as to keep the coolant temperature constant.
3. Balanced oscillator tests in which the reactivity-coolant temperature transfer function is determined for the case in which the reactivity and flow oscillations are adjusted so as to keep the power constant.

Transient tests have been analyzed for various total reactivity worths and ejection rates at different power levels. Such tests allow the reactivity-energy coefficient to be determined over a wide range of fuel temperatures.

A description of each test and of the power-temperature domain over which each test can be performed based on current SEFOR design capabilities is presented. Analytical models for the various feedback effects, together with recently calculated coefficients consistent with the SEFOR mockup tests in ZPR-3 are given. Methods developed for the evaluation of the feedback coefficients in the analytical model from the results of the static, oscillator, and transient tests are described. The proposed instrumentation, data acquisition system and data processing techniques are also described.

Contents

- 1.0 INTRODUCTION
- 2.0 REACTIVITY MODEL AND COEFFICIENTS
 - 2.1 Individual Reactivity Effects
 - 2.2 Composite Reactivity Model
 - 2.3 Reactivity Model for Oscillator Tests
 - 2.4 Calculated Reactivity Coefficients
- 3.0 DESCRIPTION OF TESTS
 - 3.1 Critical Tests
 - 3.2 Static Tests
 - 3.3 Oscillator Tests
 - 3.4 Sub-Prompt Critical Transient Tests
 - 3.5 Super-Prompt Critical Transient Tests
- 4.0 EXPERIMENTAL DOMAIN
- 5.0 EXPERIMENTAL EQUIPMENT
 - 5.1 Instrumented Fuel Assemblies
 - 5.2 Transient Power Detectors
 - 5.3 Plant Instrumentation
 - 5.4 Data Acquisition System
 - 5.5 Reactivity Control Equipment
- 6.0 DATA ANALYSIS
 - 6.1 Static Tests
 - 6.2 Oscillator Tests
 - 6.3 Transient Tests

1.0 INTRODUCTION

SEFOR (Southwest Experimental Fast Oxide Reactor) is a 20 MW(t) fast spectrum reactor fueled with $\text{PuO}_2\text{-UO}_2$ and cooled with sodium. SEFOR will be used to obtain physics and engineering data for fuel compositions, and temperatures characteristic of large fast oxide power reactors.

The SEFOR Project consists of two major parts: the design and construction of the reactor and a related research and development program. Funds for the design and construction of the facility are being provided by the Southwest Atomic Energy Associates (a group of seventeen investor-owned utility companies located in the southern and southwestern United States), together with the Karlsruhe Laboratory of West Germany, Euratom, and the General Electric Company. The United States Atomic Energy Commission is supporting the research and development program.

This report describes the present status of the pre-operational planning and analysis of the physics experiments to be performed to obtain SEFOR reactivity characteristics. Earlier descriptions of the experimental program appear in References 1 to 4.

2.0 REACTIVITY MODEL AND COEFFICIENTS

One of the feedback mechanisms of primary interest in SEFOR is the fuel Doppler coefficient. Determination of the Doppler coefficient, and most other reactivity feedback mechanisms, in an operating reactor is complicated by the fact that most practical experiments involve simultaneous changes in more than one reactivity feedback mechanism. Therefore, an analytical description of reactivity feedback must be composed of individual reactivity feedback models.

The separation of reactivity feedback effects is not exact due to errors in experimental data and lack of fundamental understanding of all feedback effects. Nonetheless, it is expected that the feedback effects described below will adequately describe the SEFOR reactivity behaviour, and that this model can be used to obtain a fit to the experimental data.

2.1 Individual Reactivity Effects

2.1.1 Doppler Effect

Calculations have shown that for SEFOR the Doppler effect, Δk_D , may be closely approximated by:

$$\Delta k_D = \frac{\int_{V_{\text{Core}}} P^2(\underline{r}) f(\underline{r}) dV}{\int_{V_{\text{Core}}} P^2(\underline{r}) dV} \quad (2-1)$$

where: P = power

$f(\underline{r})$ = a function of the change in local fuel temperature, $T_f(\underline{r})$

A local Doppler coefficient, Γ , may be defined such that:

$$f(\underline{r}) = \int_{\Delta T(\underline{r})} \Gamma dT_f = \int_{\Delta T(\underline{r})} \left[-\frac{dk}{dT_f} \right] dT_f = \Delta k_D(\underline{r}) \quad (2-2)$$

Analysis has shown that the local Doppler coefficient may be represented as:

$$\Gamma = \frac{A}{T_f^m} \quad (2-3)$$

where: A and m are constants

Substitution and integration over a change in fuel temperature gives:

$$\Delta k_D = \frac{A}{1-m} \frac{\int_{V_{Core}} P^2(\underline{r}) \Delta \bar{T}_f(\underline{r})^{1-m} dV}{\int_{V_{Core}} P^2(\underline{r}) dV} \quad (m \neq 1) \quad (2-4a)$$

where the symbol " Δ " denotes a change, or

$$\Delta k_D = \frac{A \int_{V_{Core}} P^2(\underline{r}) \Delta \ln T_f(\underline{r}) dV}{\int_{V_{Core}} P^2(\underline{r}) dV} \quad (m=1) \quad (2-4b)$$

It is also planned to represent the Doppler effect by a less complicated form that is more useful for reactor operating purposes. Calculations indicate that one of the following forms may be useful in this regard:

$$\Delta k_D = \frac{A}{1-m} \Delta \bar{T}_{eff}^{1-m} \quad (m \neq 1) \quad (2-5)$$

$$\Delta k_D = A \Delta \ln T_{eff} \quad (m=1) \quad (2-6)$$

where: T_{eff} = effective fuel temperature = $\bar{T}_c + R_f P$

and where:

\bar{T}_c = average coolant temperature

R_f = change in effective fuel temperature with respect to power

2.1.2 Fuel Axial Expansion Effect

The axial dimension of the fuel is related to the fuel temperature. Analysis of experimental SEFOR data will be based on pre-calculation of the reactivity effect of the fuel axial expansion, Δk_e .

2.1.3 Coolant Temperature Effect

It is planned to represent the primary coolant effect by:

$$\Delta k_c = C_q \Delta \bar{T}_c \quad (2-7)$$

where the coefficient C_q includes the direct coolant temperature coefficient C_c as well as temperature coefficients associated with the expansion of core structure C_m , and a portion of the clad expansion C_t .

In the event that the coolant effect is not adequately represented by the average coolant temperature coefficient above, a second coolant temperature coefficient associated with one of the other three measures of coolant temperature (inlet temperature, outlet temperature, or coolant temperature rise) will be included as a secondary reactivity effect, e.g. for the inlet temperature \bar{T}_i :

$$\Delta k_i = C_i \Delta \bar{T}_i \quad (2-8)$$

2.1.4 Fuel Cladding Effect

The temperature of the clad depends on the fuel surface temperature \bar{T}_{fs} as well as the coolant temperature. The cladding axial expansion effect may be represented by:

$$\Delta k_t = C_t \Delta \bar{T}_t = c C_t \Delta \bar{T}_{fs} + d C_t \Delta \bar{T}_c \quad (2-9)$$

where

$$c + d = 1$$

For experimental purposes $d C_t$ is included in C_q .

2.1.5 Coolant Flow Effect

The change of reactivity, Δk_w , for a change in coolant flow at constant coolant temperature is expected to be very small. This effect should be of the form:

$$\Delta k_w = C_w \Delta w \quad (2-10)$$

where C_w is the coolant flow coefficient.

2.1.6 Reflector Temperature Effect

The change of reactivity, Δk_r , for a change in the average temperature of the reflector, should be of the form:

$$\Delta k_r = C_r \Delta \bar{T}_r \quad (2-11)$$

where C_r is the reflector temperature coefficient.

2.2 Composite Reactivity Model

The reactivity model planned for the description of the total feedback reactivity change (Δk) between two reactor conditions is a combination

of the individual effects. Only those effects presently thought to be important are included. Thus:

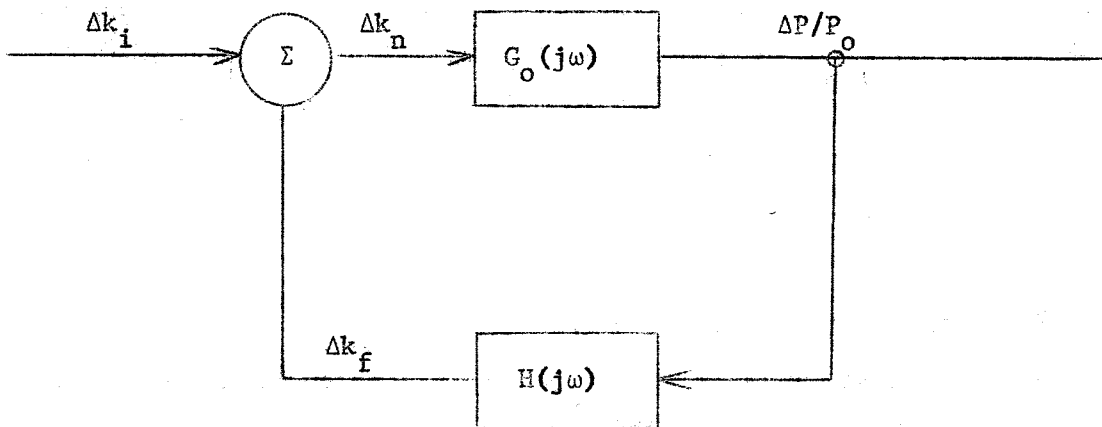
$$\Delta k = \frac{A}{1-m} \frac{\int_{V_{\text{Core}}} P^2(\underline{r}) \Delta \bar{T}_f(\underline{r})^{1-m} dV}{\int_{V_{\text{Core}}} P^2(\underline{r}) dV} + \Delta k_e + C_q \Delta \bar{T}_c + C_r \Delta \bar{T}_r + cC_t \Delta \bar{T}_{fs} \quad (2-12)$$

or using equation (2-5), the model may also be used in a simplified form when the Doppler term is of the form:

$$\frac{A}{1-m} \Delta \bar{T} (T_c + R_f P)^{1-m}$$

2.3 Reactivity Model for Oscillator Tests

Results of conventional oscillator tests are analyzed to determine the overall power-reactivity frequency response. The block diagram below shows the analytical model.



Simple Analytical Model for Oscillator Tests

The nomenclature used in the block diagram is defined below.

- Δk_i - input reactivity (oscillator) (cents)
- Δk_f - feedback reactivity (cents)
- Δk_n - net reactivity (cents)
- $\Delta P/P_o$ - percent change in reactor power

$G_o(j\omega)$ - zero power neutron kinetics frequency response $(\% \Delta P/P)/c$

$H(j\omega)$ - overall feedback frequency response $c/(\% \Delta P/P)$

Measured quantities are

$G_o(j\omega)$ - measured at zero power (0.01 MW)

$G_1(j\omega) = \frac{G_o}{1 + G_o H}$ - measured at power (≥ 0.1 MW)

Figure 2-1 shows a block diagram of a typical analytical model for SEFOR. For clarity, the model is shown for a "point reactor". Actually, the reactivity effects are distributed over the whole reactor. Possible direct effects of inlet and outlet coolant temperature on Δk have been omitted. The fuel coefficient (C_f) includes both Doppler and fuel axial expansion effects.

The nomenclature used in Figure 2-1 is defined as follows:

$G_o(j\omega)$ = zero power frequency response of neutron kinetics

$F_{av}(j\omega)$ = average fuel temperature response to power oscillation

$F_s(j\omega)$ = average fuel surface temperature response to power oscillation
(or average fuel temperature response to coolant temperature oscillation)

$F_n(j\omega)$ = average fuel surface temperature response to coolant temperature oscillation

$F_w(j\omega)$ = core temperature rise response to fuel surface temperature oscillation (essentially constant in the range 0.001 to 0.1 cps)

$F_\ell(j\omega)$ = core inlet temperature response to fuel surface temperature oscillation

$F_m(j\omega)$ = core structure temperature response to average sodium temperature oscillation

$F_r(j\omega)$ = reflector temperature response to core power oscillation (guide structure time constant 1.5 min.; segment time constant 18 min.)

The $F(j\omega)$ functions described above are normalized so that the zero frequency values are all 1.0. The "K" values associated with each $F(j\omega)$ will vary with power levels, coolant flow rate, and the method of plant control.

At a reactor power of 20 MW and full coolant flow conditions additional parameters are:

$$\begin{aligned}
 a &= 0.5 \\
 b &= 1.0 \\
 c &= 0.15 \\
 d &= 0.85
 \end{aligned}
 \quad
 \begin{aligned}
 (\Delta \bar{T}_c &= b \Delta \bar{T}_i + a \Delta \theta, \theta = \bar{T}_o - \bar{T}_i) \\
 \Delta \bar{T}_t &= c \Delta \bar{T}_{fs} + d \Delta \bar{T}_c
 \end{aligned}$$

2.4 Calculated Reactivity Coefficients

Calculations for SEFOR indicate that the Doppler power (but not temperature) coefficient will be considerably larger than the other effects. The following values have been calculated, or estimated from ZPR-III critical experiments⁽⁵⁾, for the constants that appear in the reactivity feedback model for 2-segment fuel with dished pellets.

$$\begin{aligned}
 \text{Doppler: } m &= 1.0 && \text{corresponds to } T \frac{dK_D}{dT} = -0.0085 \\
 A &= -2.58\% && \text{or at 20 MW } \frac{dK_D}{dT} = -0.109 \text{ } \ell/\text{ } ^\circ\text{F}
 \end{aligned}$$

Average Coolant temperature effect:

$$\begin{aligned}
 \text{core structure radial expansion, } C_m &= -0.183 \text{ } \ell/\text{ } ^\circ\text{F} \\
 \text{coolant density, } C_c &= -0.108 \text{ } \ell/\text{ } ^\circ\text{F} \\
 \text{clad axial expansion, } dC_t &= -0.066 \text{ } \ell/\text{ } ^\circ\text{F} \\
 C_q &= \underline{-0.357 \text{ } \ell/\text{ } ^\circ\text{F}}
 \end{aligned}$$

Fuel surface temperature effect:

$$\text{clad axial expansion, } cC_t = -0.0117 \text{ } \ell/\text{ } ^\circ\text{F}$$

Reflector temperature effect:

$$\text{reflector coefficient, } C_r = -0.04 \text{ } \ell/\text{ } ^\circ\text{F}$$

Other typical values at a reactor power of 20 MW and full coolant flow conditions are:

$$K_{av} = 11.4^{\circ}\text{F}/\% \text{ power (average fuel temperature response to power change)}$$

$$K_s = 1.9^{\circ}\text{F}/\% \text{ power (average fuel surface temperature response to power change)}$$

$$K_w = 0.63^{\circ}\text{F}/^{\circ}\text{F} \text{ (core } \Delta T \text{ response to fuel surface temperature change)}$$

$$K_l = 0.71^{\circ}\text{F}/^{\circ}\text{F} \text{ (core inlet temperature response to fuel surface temperature change)}$$

$$K_r = 0.7^{\circ}\text{F}/\% \text{ power (reflector temperature response to power change)}$$

3.0 DESCRIPTION OF TESTS

The following paragraphs describe the types of tests and the experimental domain of interest for the SEFOR reactor. The initial planning required for the specification of equipment and the description of the tests has been completed.^(3,4) The detailed selection of tests and the specifications of test conditions are now underway.

The tests have been divided into the following categories: critical, static, oscillator, sub-prompt transients, and super-prompt critical transients. In general the tests will be performed chronologically as listed, however, checks of previous results may be performed throughout the program in order to detect changes in plant characteristics.

3.1 Critical Tests

3.1.1 Dry Critical Test

The dry (no sodium) critical mass of the core at room temperature will be determined. This will be compared with the wet (sodium filled) critical mass to obtain the reactivity worth of complete sodium loss from core and vessel, which is calculated to be approximately minus ten dollars.

3.1.2 Wet Critical Tests

In addition to obtaining the wet critical mass at a sodium temperature of 400°F, it is planned that material worths (relative to sodium) of such materials as fuel, B₄C, steel, and nickel will be measured. Measurements of the fission rate distribution of Pu²³⁹ along the core axis at different radial locations are being considered.

Analysis of tests performed on the SEFOR critical mockup in ZPR-3 indicates that values of λ/β as determined by the pulsed neutron source and noise analysis methods agree quite well.⁽⁵⁾ It is planned that the noise analysis method will be used in SEFOR. The expected value of λ/β is 2×10^{-4} seconds.

3.1.2.1 External Heating

The core and coolant can be heated from 400°F to 1000°F using an external heat source. This capability will allow thermal equilibrium to be attained at several different temperatures. From measurements of the equilibrium

fuel, coolant, and reflector temperature, in addition to control rod position and neutron flux level, "isothermal" reactivity coefficients can be obtained.

In order to correct later heat balances at high power the heat losses from the reactor vessel may be determined at various temperatures by measuring sodium flow and the temperature difference between vessel inlet and outlet.

3.1.2.2 Reactivity Worth of Sodium Flow

The flow-reactivity effect is expected to be small. This expectation can be checked by changing the primary sodium flow and measuring the reactivity effect by calibrated rod. The flow can be varied over the range between 20 and 100 % of fuel flow. In addition, the flow can be oscillated at different frequencies in the range 0.0012 to 0.03 cps.

3.2 Static Tests

The primary purpose of the Static Tests is to determine the change in reactivity associated with changes in reactor power and coolant temperature between two steady state conditions. These tests can be performed by changing only one of the variables, power average coolant temperature, or inlet temperature, while the other two variables are held constant. The resultant change in reactivity between specified steady state conditions is measured by calibrated rod. By proper sequencing of the variable which is to be changed, it is possible to cover a wide range of power, average coolant temperatures, and inlet temperatures.

The reflector temperature coefficient can be measured by changing the reflector coolant flow rate while the reactor is at power.

The procedures to be used in performing the static tests are summarized below.

<u>Reactivity Coefficient</u>	<u>Variable Changed</u>	<u>Variables Held Constant</u>
(fuel + clad) power coefficient $K_{av}C_f + cC_tK_s$	P	T_r, \bar{T}_c, T_i
(coolant + fuel + clad) temperature coefficient $C_q + C_f + cC_t$	\bar{T}_c	T_r, T_i, P
inlet temperature coefficient C_i	T_i	T_r, P, \bar{T}_c
reflector temperature coefficient C_r	T_r	P, \bar{T}_c, T_i

3.3 Oscillator Tests

3.3.1 Conventional Oscillator Tests

In the conventional oscillator tests the reactivity is oscillated at fixed frequency and amplitude and corresponding changes in plant variables are recorded.

The SEFOR reactor has one-inch diameter fuel rods. This allows SEFOR to attain the high temperatures of interest for large fast oxide reactors while operating at the relatively low power level of 20 MW. This also means that SEFOR will have a large (30 sec) fuel time constant and that the frequency range of interest for the oscillator tests will be in the range 0.0012 to 0.5 cps. The amplitude of the oscillating reactivity can be varied with frequency and power level so that the power oscillation ($\Delta P/P_0$) is 5 to 10 %.

3.3.1.1 Zero Power Tests

Due to an estimated spontaneous fission plus (α, n) source of 3.0×10^{-4} watts, the reactor will be 0.3 β subcritical at 100 W. This implied that the zero power frequency response should be measured at a power level in the range 100 W to 1 kW.

It is estimated that for SEFOR (beryllium mass fraction = 0.0089) the delayed photoneutrons will cause a change in the zero power transfer function of less than 0.2 % in amplitude and 0.2 degrees in phase at 0.0012 cps.

3.3.1.2 Power Tests

Reactor frequency response measurements in the range of average power levels between 0.1 and 20 MW are of interest. For a frequency range between 0.0012 cps and 0.5 cps, the reactor steady state core temperature rise for such tests would range up to 120°F. The average fuel temperature amplitude would vary with frequency and power level between ±10°F and ±100°F.

3.3.2 Balanced Oscillator Tests

Balanced oscillator tests have been described by Caldarola⁽⁶⁾. These tests involve oscillating the input reactivity, the primary coolant flow, and the secondary coolant flow in such a manner that either: (1) the core coolant temperature is held constant (first balanced oscillator experiment), or (2) the power is held constant (second balanced oscillator experiment). The first balanced oscillator experiment allows measurement of the fuel plus clad power coefficient, while the second balanced oscillator test allows measurement of the fuel temperature coefficient (see Section 6.0).

In these tests the temperature and power reactivity effects are separated so that a frequency range of 0.0012 cps to 0.03 cps is adequate (the average fuel element time constant is ≈30 sec).

Practical methods for achieving balanced conditions are described in Reference (7).

3.4 Sub-Prompt Critical Transient Tests

The sub-prompt critical tests involve rapid insertion of less than 1.0 \$ positive reactivity. The initial fuel temperature rise is rapid so that heat conduction in the fuel is negligible during the first 1 to 2 seconds (i.e. for times small compared to the ≈30 sec fuel time constant).

Tests currently being analyzed cover the following range of conditions:

Initial power	- from 0.1 MW to 14 MW
Initial sodium temperature	- 500 to 760°F
Δk insertion	- 0.1 \$ to ≈0.95 \$
Δk insertion time	- approximately 0.1 second

The actual values of initial power and Δk insertion will be limited so that fuel does not melt.

The sub-prompt critical transients of interest can result in peak power levels of 10 to 20 times the initial power and a maximum temperature rise in the average fuel of 100 to 150°F at rates up to 200°F/sec. At full coolant flow the maximum clad and sodium average temperature rises are approximately 20°F and 10°F, respectively. The cladding and sodium temperature rises during the first few tenths of a second are due primarily to direct gamma and neutron heating.

3.5 Super-Prompt Critical Transient Tests

The super-prompt critical tests involve rapid insertion of more than 1.0 % positive reactivity. Maximum transients of this type will result in peak power levels of 10^4 to 10^5 times the initial power and a maximum temperature rise in the average fuel of less than 1000°F at rates approaching 10,000°F/sec. The reactivity effects due to cladding and sodium temperature rise may be 15 % of the fuel reactivity effect.

Tests using Δk insertion in the range 1.0 % to 1.5 % in approximately 0.1 second are of primary interest, since these results in significant fuel temperature rise independent of heat conduction effects. An error analyses indicates that little increase in accuracy can be obtained by using Δk insertions >1.5 %.

Tests currently being analyzed cover the following range of conditions:

Initial power	- from 0.1 MW to 12 MW
Peak power	- 10^3 to 10^5 MW
Period range	- 0.1 to 0.001 second
Δk insertion	- 1.0 % to 1.5 %
Δk insertion time	- approximately 0.1 second
Initial sodium temperature	- 500 to 760°F

The actual values of initial power and Δk insertion will be limited so that fuel does not melt.

4.0 EXPERIMENTAL DOMAIN

It is desired to evaluate and determine the validity of the reactivity model over a wide range of reactor operating conditions. The operating characteristics of SEFOR have been determined using 1) recently calculated fuel temperatures, 2) the coefficient values listed in Section 2.4 (excluding C_r), and 3) a fuel axial expansion model, $\Delta k_e(\phi) = -0.0149 \Delta \bar{T}_c - 0.44 \Delta P$. The resulting SEFOR characteristics are shown in Figure 4-1 as the change of k versus the average temperature of the coolant, along lines of constant power. In Figure 4-2 the characteristics are shown in terms of the average temperature of the fuel rather than the average temperature of the coolant.

A desirable range of operating conditions over which test data may be obtained must be consistent with reactor capabilities, and safety considerations. The range, or experimental region, that is being used for planning the SEFOR tests was obtained using the reactor characteristics shown in Figures 4-1 and 4-2, and the following considerations:

- a) primary and secondary coolant system flows are equal,
- b) 400°F minimum coolant temperature in secondary coolant loop,
- c) 1000°F maximum core outlet temperature,
- d) average temperature of the fuel not to exceed the value at 20 MW and full flow operation (i.e. the maximum fuel temperature remains below the melting point).

The resulting experimental region is shown in Figures 4-1 and 4-2 as the area enclosed in the dotted lines. The static and oscillator tests, as well as the initial conditions for the transient tests lie within this region.

AVERAGE COOLANT TEMPERATURE, \bar{T}_c - °F

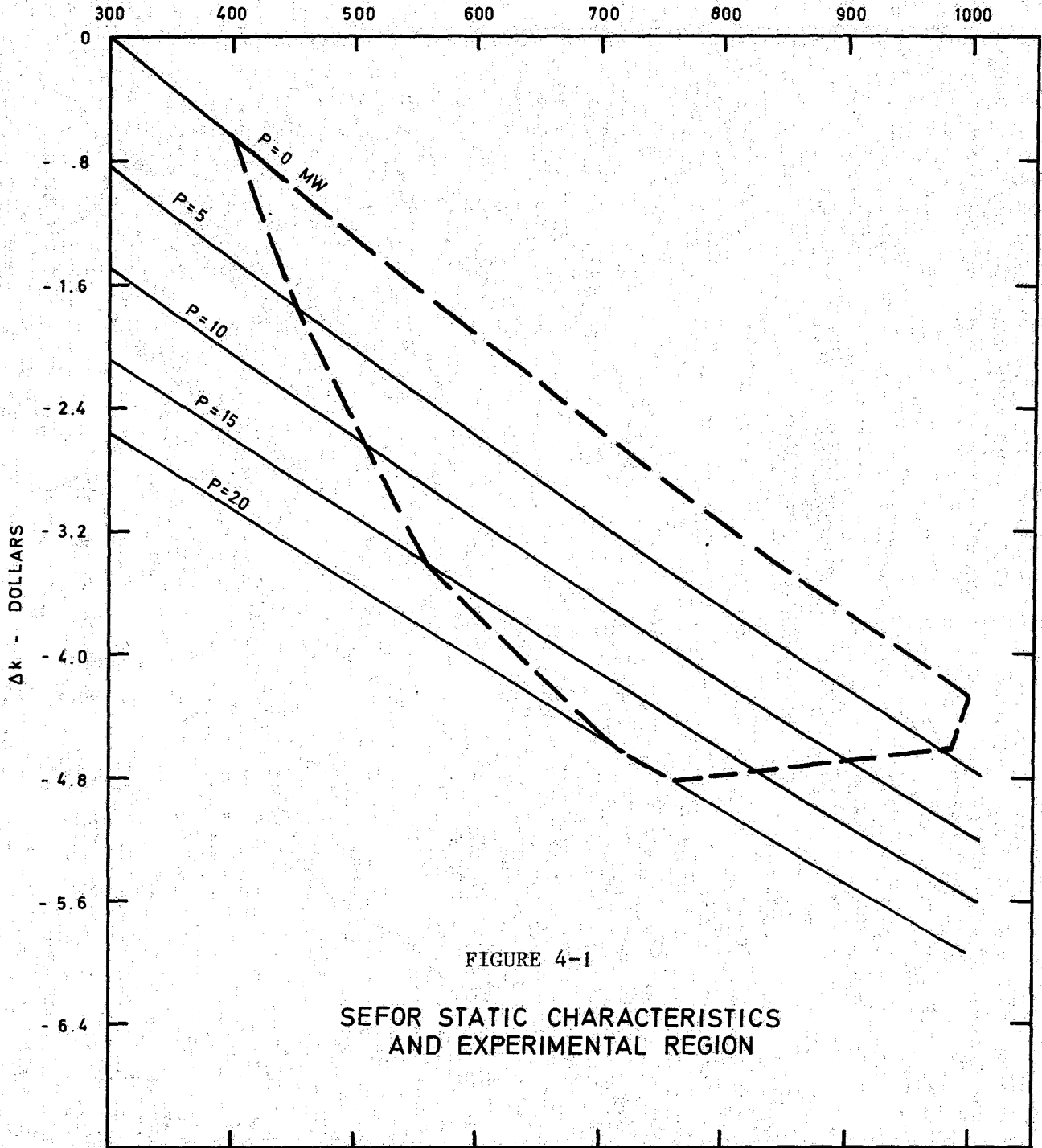
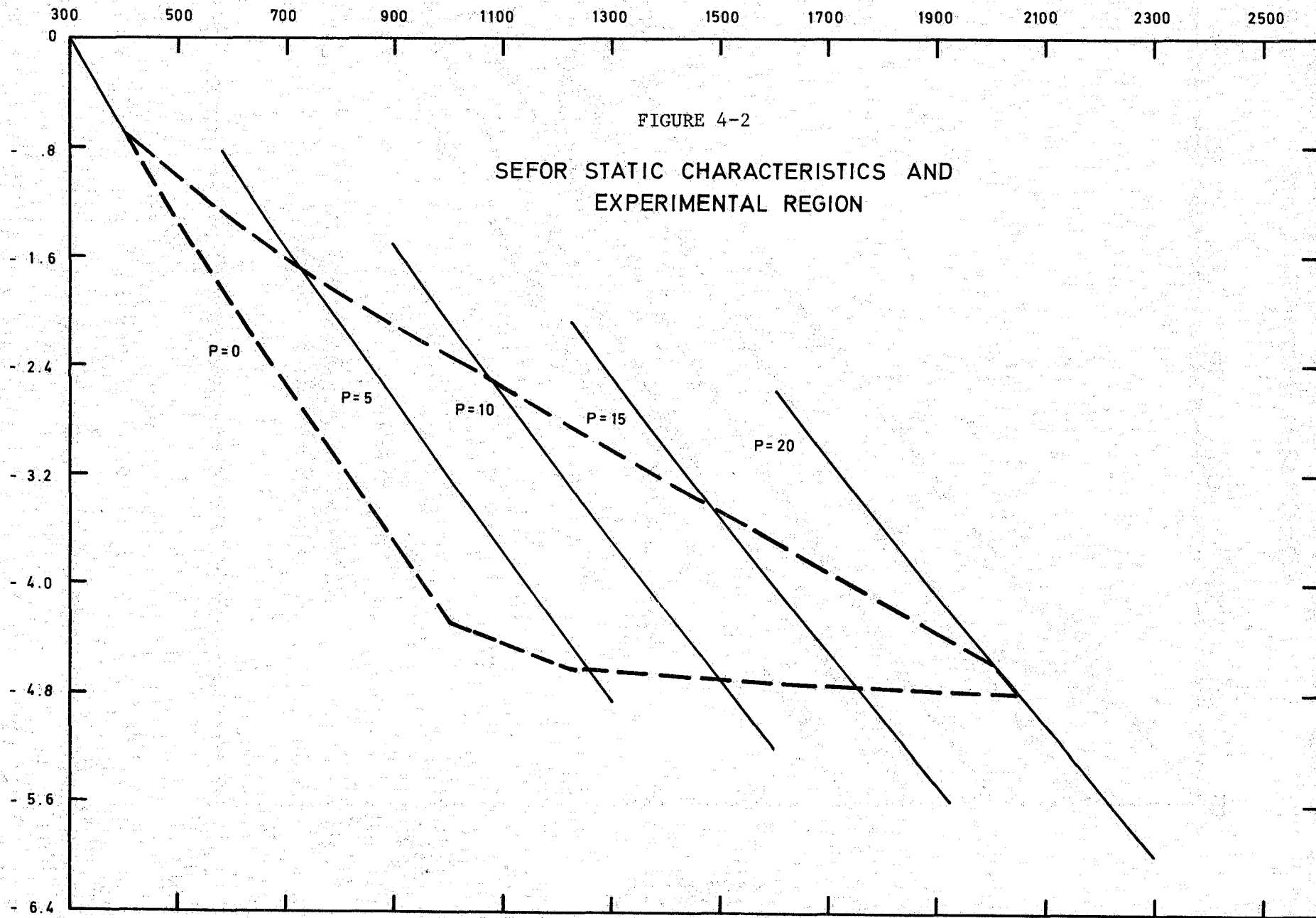


FIGURE 4-1

SEFOR STATIC CHARACTERISTICS
AND EXPERIMENTAL REGION

AVERAGE FUEL TEMPERATURE, \bar{T}_f - °F



5.0 EXPERIMENTAL EQUIPMENT

5.1 Instrumented Fuel Assemblies

The instrumented fuel assemblies provide data on fuel and coolant temperatures and coolant flow for both analysis and test operations purposes. Each assembly contains fuel and coolant thermocouples and a coolant flowmeter. There are six positions in the SEFOR core in which the instrumented fuel assemblies can be placed. These positions provide for two assemblies at each of three radial locations.

Each instrumented fuel assembly will contain two special fuel rods with two tungsten-rhenium fuel thermocouples in each rod. Approximately 12 % of the normal fuel volume has been removed from the 6-fuel rod fuel assembly to provide space for the thermocouples and lead wires. One thermocouple in each rod will be located at the core mid-plane while the other will be at the approximate average axial power position. These fuel thermocouples will be located at the radial center of the fuel rod, and inserted 3 inches into the top of a fuel column so that axial heat conduction effects are negligible. The thermocouples are not intended to follow the most rapid of the planned transient tests, however they should indicate the maximum transient center fuel temperature. An extensive series of in-pile and out-of-pile tests have been performed in the process of developing a suitable fuel thermocouple design. These tests have included: (1) transient tests, (2) steady state calibration tests, (3) tests to determine compatibility of sheath material and mixed oxide fuel, and (4) determination of gamma and neutron irradiation effects on thermocouple and insulator materials.

Each instrumented fuel assembly will contain one chromel-alumel coolant thermocouple at the inlet and two at the exit. The exit thermocouples are located 6 inches above the fuel channel exit where calculations indicate a 10^oF variation in the coolant temperature due to "channeling" effects. The coolant thermocouple time constant is estimated to be 0.1 second in the flowing sodium environment.

Coolant flow in each channel will be measured by a permanent-magnet flowmeter mounted at the channel inlet. The flowmeters replace the normal channel orifice and develop approximately 10 millivolts at full flow. Flowmeter calibration has been performed in a simulated reactor sodium flow configuration.

5.2 Transient Power Detectors

The purpose of the transient power detectors is to provide a record of the reactor power transient which can be used for later determination of (1) instantaneous power, (2) transient energy release, and (3) instantaneous net reactivity.

A combination of neutron and gamma-sensitive detectors together with fast response logarithmic/linear amplifiers will be used to cover the transient power range from 10^{-1} MW to 10^6 MW. For design purposes, a minimum period of 1.0 millisecond has been used to establish the overall time response of the power recording channel. Using the rule-of-thumb established by the SPERT Project⁽⁸⁾, the resulting channel bandwidth is 16,000 cps. Prototypes of the ion chambers and amplifier have been built and extensive tests are scheduled to begin in the near future.

A large (3-inch O.D. x 16-inch long), gamma-compensated, U^{238} fission chamber located in the inner shield region has been chosen for the power range from 10^{-1} MW to 6×10^3 MW. The maximum measurable power is determined by the maximum chamber current of 10^{-2} amperes, while the minimum measurable power is set by the amplifier frequency response characteristics at low current. The lower limit inherent in the chamber itself is believed to be approximately 10^{-3} MW as determined by cable leakage and noise considerations. Assuming 95 % gamma compensation, calculations show that 98 % of the signal at steady state is due to components which should follow the instantaneous transient power.

For the power range 10^2 MW to 10^6 MW, a small (0.25-inch O.D. x 3-inch long) gamma sensitive chamber located at the inner reflector surface has been selected. The maximum measurable power is determined by the maximum chamber current of 3×10^{-2} amperes. The minimum measurable power depends on the allowable delayed gamma contribution. Assuming that the delayed gamma current can be no more than 2 % of the total current, then the minimum measurable power is calculated to be approximately 5 times the initial power on the rising part of a transient, and 1,000 MW on the decreasing part of a typical transient.

The reactor design provides 3 holes around the periphery for the large U^{238} chambers and 3 holes at the inner reflector surface for the small gamma

chambers. Initially, it is planned to install two U^{238} chambers in diametrically opposite positions, and two gamma chambers in corresponding reflector positions. Coupled with the log/linear amplifiers, this will provide two power recording channels for the complete range of transient power. The gamma-sensitive chambers will be calibrated by overlapping the transient records of the neutron and gamma sensitive detectors.

Although other transient reactor test projects (KEWB, SPERT, KUKLA) have consistently used linear amplifiers for power recording, it was decided to pursue the development of a wide-band logarithmic amplifier in order to reduce the number of recording channels and make the data handling process easier. A fast response, feedback amplifier was designed to convert the ion chamber currents to a voltage signal suitable for recording. The selection of either linear or logarithmic feedback is made by use of remotely operated reed switches. There are three linear ranges covering one decade each, and one logarithmic range which covers 4.5 decades. The output rise time for a step input current is less than 10 microseconds. Current measurements of the order of 10^{-7} ampere are practical on the lowest range. The amplifier uses an input buffer stage to reduce the input impedance so that the combination of cable capacitance and input impedance does not limit the response of the amplifier.

It is recognized that a given fractional error in the logarithmic recording causes a larger fractional error in the linear power which is inferred from the logarithmic record. However, it is believed that by calibrating the recording channels before each test and using direct digital recording, the overall recording error in the linear power can be made less than 5 % (this includes time response and noise as well as drift and calibration errors), but does not include errors in heat balance.

5.3 Plant Instrumentation

In addition to the instrumented fuel assemblies and transient power detectors discussed previously, some reactor plant instrumentation will provide necessary test information. The operational measurements of neutron flux, control rod position, reactor inlet and outlet coolant temperature, reactor coolant flow, and reflector temperature will be recorded as part of the test data.

The operational neutron monitors will provide a linear signal for recording at power levels above 10 watts. In addition, a visual differential neutron flux display will be provided with a resolution of 0.1 % of the full scale range at power levels above 10 watts.

The fine reflector control rods (used for shimming) will have a visual position indicator with a resolution of 0.01 inch, which corresponds to approximately 0.1 ϕ at the maximum rod incremental worth. The control rod positions will be recorded manually as needed for each test.

The coolant temperatures indicated by the resistance temperature detectors at the vessel inlet and exit will be recorded. This data will be used in conjunction with core flow data to determine the reactor power level and to check the in-core coolant thermocouples. The temperature detectors should indicate the reactor coolant ΔT with less than $\pm 3^{\circ}\text{F}$ error. This results in a calculated reactor power error of less than $\pm 5\%$. The temperature detectors are estimated to have a 5 to 8 second time constant, so that they are expected to be used only for static test measurements and not in the oscillation or transient tests.

A Venturi flowmeter will be installed in the primary system along with an electromagnetic flowmeter for the purpose of measuring reactor coolant flow. The Venturi meter will be calibrated in water prior to installation, and it is planned to measure full reactor flow with $\pm 2\%$ error.

It is planned to record temperatures at several points in the reflector structure and movable segments. This data will be used in determining the effect of reflector temperature changes on reactivity.

5.4 Data Acquisition System

The purpose of the data acquisition system is to provide accurate records of the various tests which can be conveniently used for on-site test guidance and later extensive analysis. The system is planned to be capable of performing limited on-site data processing as well as the recording function. In general, this on-site processing will include:

- a. conversion of raw data to engineering units for all tests;
- b. Fourier analysis to determine the fundamental frequency components of two channels during the frequency response tests;

- c. synthesis of complete transient records for fast transient tests; and
- d. preparation of data in a form suitable for more extensive analysis at the GE-San José site.

Rather than accomplish these tasks by a variety of special purpose systems, it seemed attractive to consider a general purpose digital system. It was determined that commercially available components could be combined in a computer-controlled system to perform all the desired on-site functions. The computer controls the scanning, digitizing and data storage operations during tests, and is used after the tests to perform limited data processing.

Basically, the data acquisition system consists of the following components:

Solid state scanner

Analog-to-digital converter (11 bits plus sign)

Computer with 8,000-word core storage (16 bits per word)

Teletypewriter with paper tape punch and reader

Two digital magnetic tape units

Calibration unit

Digital incremental graph plotter

Analog recorders for on-line use (pen-type and light-beam oscillographs)

The basic system operates at a 30,000 samples per second rate in the analog-to-digital conversion unit. The digitized data are written on one digital magnetic tape unit at 40,000 samples per second. It is planned to scan and record 72 channels of low-speed data (thermocouples and flowmeters) at 140 samples per second per channel. Only two of the four fast response transient power detector channels (ion chamber-log amplifier system) will be recorded at a rate of 10,000 samples per second per channel. The scanner will switch from the neutron sensitive chamber to a gamma-sensitive chamber (and vice-versa) when a pre-set input signal level is reached. The system makes one scan through a total of 74 variables in 7.4 milliseconds, with time information included in each group of 74 data words. This format is fixed for all tests and the effective sampling rate per channel is changed by changing the time interval between successive scans of all the variables. Thus, for the static tests all variables are scanned and recorded every minute, or on command of the operator. The scanning rate is increased as needed for the frequency response and transient tests. In order to provide guidance for the frequency response tests,

the computer will perform a Fourier analysis of two channels during the tests and print out Fourier component values evaluated for the frequency of oscillation.

Continuous recording will be available for selected channels by use of a 6-channel light-beam oscillograph and a 12-channel pen-type oscillograph. A 100-channel multi-point recorder will be available for trend recording as a check on the long-term behaviour of the sensors. The digital plotter will be used to check the stored data after the frequency response and transient tests. Static test data will be printed out on the teletypewriter after conversion to engineering units.

The channel sampling rates have been chosen⁽⁹⁾ by considering the dynamic characteristics of the data, and the data analysis which is to be performed after the tests. It is recognized that unwanted "noise" in a data channel at frequencies higher than one-half the sampling rate can cause errors in reconstructing the data from the samples. Pre-sampling filters are included in all channels to eliminate high frequency noise, and if necessary the basic sampling rate can be increased from 30,000 samples per second to 60,000 samples per second by adding a second analog-to-digital converter. The most likely noise frequency is 60 cps, so that the maximum sampling rate of 140 samples/sec/channel for the slow transient data (thermocouples) and 10,000 samples/sec/channel for the fast transient data (ion chambers) should be adequate. However, electronic filtering of the signals to eliminate unwanted high frequencies may be necessary if it is desired to take data at sampling rates slower than the maximum rates.

5.5 Reactivity Control Equipment

Two special items of experimental reactor equipment have been designed for producing the reactivity changes which are necessary for the oscillation and transient tests. Both the rod oscillator and fast reactivity excursion device are designed to be placed (not simultaneously) in the central dry well in the SEFOR core. Both devices are mounted on the same positioning drive which allows the initial position of the poison material to be varied over the upper half of the core with approximately 0.1-inch increments.

The rod oscillator has a sinusoidal position versus time characteristic which is produced by a variable-amplitude scotch yoke mechanism. The oscillation amplitude and frequency are continuously variable over a range of ± 0 to ± 4.5 inches and 0.00125 cps to 0.5 cps, respectively. A maximum reactivity change of $\pm 10 \text{ } \phi$ can be achieved with a 30 ϕ total worth poison rod. The rod position is indicated and recorded by the data acquisition system using a variable inductance linear transducer with a resolution of 0.01 inch. In addition, a selsyn transmitter is driven by the rotating scotch yoke mechanism for the purpose of balanced oscillator test control. It is possible to statically position the oscillator rod at any point over the stroke in order to measure the reactivity versus position characteristic.

The fast reactivity excursion device is a gas-actuated device capable of ejecting a poison rod from any axial position in the upper half of the core in a time interval which is variable from 0.050 to 0.150 seconds. The poison rod is allowed to return to its initial position approximately 1 to 5 seconds after ejection. Tests have shown that the rod ejection time is reproducible within $\pm 2.5 \%$ of the ejection time. The poison device position is indicated and recorded by the data acquisition system using 3 magnetic switches indicating lift-off, mid-point of in-core travel, and core exit. In addition, a photoelectric device indicates the motion of the device by registering the passage of alternate dark and light bands past the photocell. The fast reactivity excursion device uses different poison worths and has the capacity to provide reactivity increments over the range from 0.10 $\$$ to 1.50 $\$$.

6.0 DATA ANALYSIS

Pre-operational analysis of the SEFOR reactor indicates that reactivity changes will be primarily dependent upon the Doppler effect and the average coolant and structure temperature. If measurements show that the effects of inlet, clad, and reflector temperature changes are indeed small it is planned that these effects will (when necessary) be applied as corrections to the measured feedback. The "corrected reactivity" will then be used to determine the dependence of the Doppler effect (ΔK_D) and the average coolant temperature coefficient C_q upon power (or energy) and average coolant temperature. It is planned that the necessary correction for the fuel axial expansion effect (which should be small because of SEFOR fuel design) will be calculated rather than measured.

The Doppler effect may be determined by using the simplified model given in (2-5) or (2-6), and/or by using the more complicated model described by (2-1). If the simple model is used, calculations can be performed to determine the expected dependence of the parameter R_f upon the coolant temperature, power, and transient energy release. These calculations can then be compared with the actual experimental results of the various tests.

If the latter procedure is used, the spatial power and fuel temperature distribution, as well as an assumed form for $f(\underline{r})$ must be used in equation (2-1). The spatial power and temperature distributions can be obtained from calculations based on measurements of spatial fission distributions and fuel temperatures in the instrumented fuel assemblies. The parameters in the assumed form for $f(\underline{r})$ (such as A and m in 2-2) can then be adjusted so as to obtain the best least squares fit to the measured dependence of ΔK_D upon power and coolant temperature.

6.1 Static Tests

The power coefficient, $C_{f_{av}} + cC_{t_s}$, can be obtained from the static tests in which the power is changed and the coolant temperatures are held constant. After correction for secondary effects the "static" change in reactivity due to a change in average coolant temperature at constant power will involve the temperature coefficients $C_f + cC_t$, and C_q . A least squares fit of the reactivity model to this experimental data can be performed to determine the "best" values of the model parameters.

6.2 Oscillator Tests

It is planned that the reactivity transfer functions will be obtained by treating the oscillating signal outputs in the manner described by R. Persson⁽¹⁰⁾. This technique is similar to a Fourier analysis except that the signal is multiplied by a square wave whose amplitude during successive half cycles varies as the binomial coefficients. This technique helps to eliminate "drift" and our analysis has shown that any "white" noise contribution decreases as 2^{N-1} rather than as $1/N$ in the "conventional" method.

6.2.1 Conventional Oscillator Tests

It is planned that the feedback response, $H(j\omega)$, will be least squares fitted to the model described in Section 2.3, and/or to a simplified form of it. For SEFOR, $H(j\omega)$, in the frequency range 0.001 to 0.1 cps, is approximately the sum of the fuel, clad, structure, and sodium power coefficients multiplied by the average fuel temperature response to power oscillation $F_{av}(j\omega) \approx 1/(1+j\omega\tau_f)$, where $\tau_f = 30$ sec is the fuel time constant. At higher frequencies $G_o(j\omega)$ and $G_1(j\omega)$ are nearly identical. This implies that it may be difficult to separate the various reactivity coefficients using only conventional oscillator techniques.

6.2.2 Balanced Oscillator Tests

The first balanced oscillator test allows measurement of two transfer functions. One transfer function, that between primary coolant, W , and power, P , has been shown⁽⁶⁾ to be equal to that between fuel surface temperature, \bar{T}_{fs} , and power.

That is

$$\frac{\Delta W(j\omega)/W_o}{\Delta P(j\omega)/P_o} = F_s(j\omega)$$

The other transfer function is that between power and reactivity

$$H(j\omega)|_{T_c} = C_f K_{av} F_{av}(j\omega) + c C_s K_s F_s(j\omega)$$

An additional transfer function which can be measured, using the fuel thermocouples, is that between power and central fuel temperature, $F_c(j\omega)$. Since F_c is related to $F_{av}(j\omega)$ and $F_s(j\omega)$ by the fuel frequency response

model⁽⁶⁾, this measurement provides another means of checking the validity of the model.

In the second balanced oscillator experiment the net reactivity is zero and one thus obtains (after any necessary corrections due to an imperfect balance)

$$\frac{\Delta K_1(j\omega)}{\Delta T_c(j\omega)} = C_c + dC_t + C_m F_m(j\omega) + cC_t F_n(j\omega) + C_f F_s(j\omega)$$

For SEFOR, $F_m(j\omega)$ is nearly equal to 1.0 in the frequency range 0.0012 to 0.1 cps. Thus, a least squares fit to the experimental values of $\Delta K_1(j\omega)/\Delta T_c(j\omega)$ yields the constant term $C_q = C_c + dC_t + C_m$ and the coefficient of the frequency dependent term $C_f + cC_t$. If the frequency dependence of F_n and F_s are significantly different it may be possible to separately determine the coefficients C_f and cC_t , since $F_s(j\omega)$ should be known from the first balanced oscillator experiment.

The values of C_f , cC_t , C_q , and $C_f K_{av} + cC_t K_s$ can be obtained at a number of power levels and average coolant temperatures and the dependence of these parameters on power and temperature can thus be experimentally determined. In particular, this data can be least square fit in order to determine the "best" values of the parameters (such as A and m) in the Doppler models described above.

6.3 Transient Tests

As in the oscillator tests, the transient analysis is based on the assumption that the "point reactor" kinetic equations are valid and that the delayed neutron parameters and λ/β are known.

In order to investigate transient spatial effects, the ramp ejection in 50 msec of poison slugs worth ~ 0.95 % have been simulated with the VARI-QUIR computer code. The results indicate that the maximum change in spatial power shape during the transients is approximately 1 % in a region immediately adjacent to the poison. The change in the group 1 flux ($E_n \geq 0.5$ MeV) divided by the average power, was ≤ 0.2 % at the U^{238} detector location. Any spatial changes in the gamma flux, at the gamma detector location should be small, since the fraction of the gamma flux arising from low-energy neutron capture is small. Thus, spatial effects should not invalidate the "point reactor" model.

Calculations have shown that the effectiveness of the individual delayed neutron groups is (within 1 %) constant. The validity of the assumed values for the delayed neutron parameters, as well as possible effects due to reflected neutrons, can be analyzed by comparing calculated and measured transients during the time interval before appreciable feedback occurs. This comparison can be made for transients resulting from the ejection of various poison worths at low initial power level.

In view of the above discussion, it is therefore planned that the net reactivity will be calculated from the flux transient by using the "point" kinetic inversion method. After smoothing the power data in a manner similar to that used at the SPERT Project, the dependence of the reactivity feedback upon the energy (time integrated power change) release will be determined.

6.3.1 Sub-Prompt Critical Tests

In these tests, the input reactivity, $\Delta K_{in}(t)$, is completely inserted in a time $t_1 \approx 0.1$ sec. Therefore, for times $> t_1$, the only change ($\delta K_{net}(t) \equiv \Delta K_{net}(t) - \Delta K_{net}(t_1)$) in the net reactivity, $\Delta K_{net} = \Delta K_{in} + \Delta K_{fb}$, will be due to changes in the feedback reactivity, ΔK_{fb} . In SEFOR most of the feedback occurs during times $> t_1$. Thus, analysis of δK_{net} , rather than ΔK_{net} , eliminates the large error in ΔK_{fb} ($0 \leq |\Delta K_{fb}| \lesssim 10 \phi$) which could occur as a result of a small error in ΔK_{in} ($0 \leq \Delta K_{in} \lesssim 95 \phi$).

For the sub-prompt transients the dependence of feedback upon the energy release, $\Delta E(t)$, should be nearly linear, i.e. $\Delta K_{fb} = \gamma \Delta E$. The dependence of the energy coefficient, γ upon the initial power, P_0 , can be determined by performing the transients from several different initial power levels.

Using calculated values of heat capacities, and of the fuel and clad expansion effects, a comparison can be made with the doppler temperature coefficient obtained from the static and oscillator experiments.

6.3.2 Super-Prompt Critical Tests

The super-prompt transients will be analyzed in a manner similar to the sub-prompt transients, and the energy dependence of the reactivity feedback will be determined for various initial power levels and for poison slug worths up to approximately 1.5 β . In addition, approximate methods such as

those described by Häfele⁽¹¹⁾ can be used for some of the transients, since the power peak should occur on the linear portion of the time dependent S-shaped reactivity input curve.

REFERENCES

1. W. HÄFELE, K. OTT, L. CALDAROLA, W. SCHIKARSKI, K.P.COHEN, B.WOLFE, P.GREEBLER, and A.B.REYNOLDS; "Static and Dynamic Measurements of the Doppler Effect in an Experimental Fast Reactor", Geneva Conf., 1966. A/Conf./28/P/644.
2. B.WOLFE, K.HIKIDO, K.HORST, and A.B.REYNOLDS, "SEFOR - A Status-Report", ANS-100, Fast Reactor Technology, National Topical Meeting, Detroit (1965).
3. G.R.PFLASTERER, "SEFOR Task 1.1 Topical Report, Specifications for the Plant and Experimental Equipment", GEAP-5092, Vol. I.
4. G.R.PFLASTERER and L. CALDAROLA, "SEFOR Task 1.1 Topical Report, Test Descriptions", GEAP-5092, Vol. II.
5. R.L.McVEAN, A. WEITZBERG, R.W.GOIN, J.A.KREMSER, and A.M.LERIDON, "Critical Assembly Mockup of SEFOR Reactor in ZPR-3", International Conference on Critical Experiments and Their Analysis, Argonne, Illinois, (October, 1966).
6. L. CALDAROLA, KFK-253, "The Balanced Oscillator Experiment"; IAR-Notiz Nr. 10, Karlsruhe, Germany, "First Balanced Oscillator Experiment"; IAR-Notiz Nr. 17, Karlsruhe, Germany, "Second Balanced Oscillator Experiment".
7. M. AUDOUX, L. CALDAROLA, P. GIORDANO, H. ROHRBACHER and C. RUSSELL, "The Balanced Oscillator Tests in SEFOR", International Conference on Critical Experiments and Their Analysis, Argonne, Illinois (October, 1966).
8. A. A. WASSERMAN, "Investigations into Distortion of Power-Burst Shape as a Function of Bandwidth and Initial Power", IDO-16480, December 19, 1965.
9. L.W.GARDENHIRE, "Selecting Sampling Rates", ISA Journal, p. 59-64, April, 1964.
10. R.PERSSON, "Method of Eliminating the Aperiodic Pattern of a Fourier Analysis, for Example in Measurements with a Pile-Oscillator", AEFI-54, Sweden (1957), English Translation - ANL-TRANS-43 (1964), Argonne, Illinois.
11. W. HÄFELE, "Prompt Supercritical Power Excursions in Fast Reactors", Nukleonik 5, 201 (1963).

ACKNOWLEDGEMENTS

We would like to acknowledge the work of the SEFOR project staff and other supporting personnel, which provided the background for the summary of the reactor experimental equipment development reported in this paper. In particular, we wish to acknowledge the work of E. R. Craig (instrumented fuel assemblies); J. T. Cochran (coolant flowmeters); E. E. Goodale, J. P. Neissel, and M. B. Wittry (ion chambers and amplifiers); P. E. Novak (fuel thermocouples); and E. R. McKeehan (rod oscillator and fast reactivity excursion devices).